NUCLEAR STRUCTURE -- THEORY

NEW CALCULATION OF THE PNC MATRIX ELEMENT FOR THE $J^\pi T$ 0^+1, 0^-1 DOUBLET IN ^{14}N

M. Horoi, G. Clausnitzer[a], B.A. Brown and E.K Warburton[b]

The aim of this contribution is to provide a new analysis of the PNC matrix element in ^{14}N based on a new Hamiltonian recently obtained by Warburton and Brown [5] and including also $3\hbar\omega$ and $4\hbar\omega$ configurations. This analysis is of importance for the support of the PNC experiments in ^{14}N [3,4] and to better understand how to improve the Hamiltonians for a more reliable description of the weak observables in light nuclei (A = 10-22). In order to investigate the sensitivity to various aspects of the truncation and interaction, we have carried out the PNC calculation for ^{14}N using wave functions obtained with a variety of assumptions.

The PNC matrix element has been calculated in a one-body approximation. In this paper we have not used the one-body PNC potential derived in the Fermi gas model approximation (see Eqs. 17-20 of Ref. [1]). Instead, we have used an exact calculation of the one-body (OB) contribution to the PNC matrix element

$$< J^\pi T \mid V_{PNC} \mid J^{-\pi} T' >_{OB} = \sum_{n_1 l_1 j_1, n_2 l_2 j_2, t} \frac{C^{T' \; t \; T}_{M' \; \tau \; M}}{\sqrt{(2J+1)(2T+1)}}$$

$$\times < n_1 l_1 j_1 \parallel U^{(0t)}_{s.p.} \parallel n_2 l_2 j_2 > OBTD((n_1 l_1 j_1)(n_2 l_2 j_2); 0t) \qquad (1)$$

where OBTD denotes the one-body-transition density and

$$< \alpha \mid U_{s.p.} \mid \beta > = \sum_{\delta \in core} [< \alpha\delta \mid V_{PNC} \mid \beta\delta > - < \alpha\delta \mid V_{PNC} \mid \delta\beta >] \; , \qquad (2)$$

is assumed. For ^{14}N, an interpolation between a ^{12}C core and a ^{16}O core has been performed. This method has been checked by comparing the one-body calculations (OB) with the full two-body (TB) calculations (see Table 1. *a* and *c*). The OB calculations give results with a precision of 2%, at least for the components of the V_{PNC} with the largest contribution to the matrix element.

The PNC matrix elements calculated with weak-coupling constants from different quark models are presented in Table 1. The isotensor contribution has been calculated in the full TB approximation and is found to give about a 7% destructive contribution to the isoscalar matrix element. In all calculations discussed below this contribution has been added to the OB result. An important way to analyse the PNC matrix element is to consider different $n\hbar\omega \rightarrow (n \pm 1)\hbar\omega$ contributions. For such an analyses we have carried out calculations with various strong Hamiltonians and different methods to treat the effect of the higher $n\hbar\omega$ configurations. We have performed different calculations (see also the code labels in Table 1):

a - The WBT interaction [5] with the SPE modified as discussed above and with (0+1+2+3)$\hbar\omega$ configurations included.

b - Same as *a* except that $4\hbar\omega$ configurations are also included for the 0^+1 states.

c - The WBT interaction with a modified $0p - 1s0d$ gap ($\Delta\epsilon_{0p} = 0.9$ MeV, $\Delta\epsilon_{1s0d} = -1.1$ MeV) and with (0+1+2+3)$\hbar\omega$ configurations included.

d - The WBT interaction with $\Delta\epsilon_{0p} = \Delta\epsilon_{1s0d} = 0$ and the $4\hbar\omega$ configurations included and shifted down by 4 MeV.

Cases *b* and *d* include the $4\hbar\omega$ configurations in the structure of the (0^+1) states. Method *d* has been designed to give a correct description of the experimental difference between the lowest (0^+1) level and the second (0^+1) level (≈ 6.5 MeV). The small shift ($\Delta\epsilon_{0p} = \Delta\epsilon_{1s0d} = 0$) necessary to correctly describe the (0^+1) levels signifies that the $n\hbar\omega$ catastrophe effect is almost healed for ^{14}N when the $4\hbar\omega$ configurations are included.

The calculated PNC matrix elements are presented in Table 1. The range of values for the DDH weak-coupling constants vary between 0.232 and 0.764 eV, with a average value of around 0.48 eV.

We have estimated the effect of the nearly unbound $1s_{1/2}$ WS state on the dominant $0p_{1/2} \rightarrow 1s_{1/2}$ contribution to the PNC matrix element. The $1s_{1/2}$ proton level is unbound by 0.4 MeV in ^{13}N and is slightly bound by 0.1 MeV in ^{17}F. For neutrons, the same level is bound by 1.9 MeV in ^{13}C and by 3.25 MeV in ^{17}O. We have chosen a -0.1 MeV value for the $1s_{1/2}$ proton SPE and -2.0 MeV for the neutron SPE. The comparable values for the $0p_{1/2}$ orbit are -2.5 MeV for protons and -5.0 MeV neutrons. The WS SPWF are obtained by adjusting the WS well depth to reproduce the above binding energies. we have found a suppression of the dominant $0p_{1/2} \rightarrow 1s_{1/2}$ contribution to the PNC matrix element of 37% in the case of protons and 28% for neutrons, an average of 32%. All matrix elements in Table 1 have to be decreased by this factor.

Table 1. Magnitude of the PNC matrix element calculated with the various strong interactions [5], different model spaces, and different models of the weak-coupling constants (see Ref. [2] for the weak interaction notation and references). Units are eV. Code labels are further explained in the text.

Interaction	Code	Model space	PNC	Weak-Coupling Models			
				DDH	AH	DZ	KM
WBT	*a*	(0+1+2+3)$\hbar\omega$	OB	0.487	0.372	0.421	0.278
	a	(0+1+2+3)$\hbar\omega$	TB	0.483	0.366	0.413	0.269
	b	(0+1+2+3+4)$\hbar\omega$	OB	0.233	0.164	0.190	0.127
	c	(0+1+2+3)$\hbar\omega$	OB	0.764	0.565	0.620	0.418
	c	(0+1+2+3)$\hbar\omega$	TB	0.732	0.549	0.620	0.400
	d	(0+1+2+3+4)$\hbar\omega$	OB	0.797	0.593	0.669	0.436

In conclusion, new calculations of the predominantly isoscalar PNC matrix element between the $(0^+1)_2, (0^-1)_1$ states in ^{14}N have been performed in a (0+1+2+3+4)$\hbar\omega$ model space using new Hamiltonians. A new method to calculate the PNC matrix elements in an one-body approximation has been proposed and shown to give reliable results as compared with the full two-body calculations; this method proves to be very useful for calculations in larger model space, e.g. (0+1+2+3+4)$\hbar\omega$. The most reasonable range of values for the PNC matrix element was found to be 0.22 to 0.54 (a 32% WS suppression included), which is in agreement with a magnitude of about 0.38 ± 0.28 eV deduced from experiment [4].

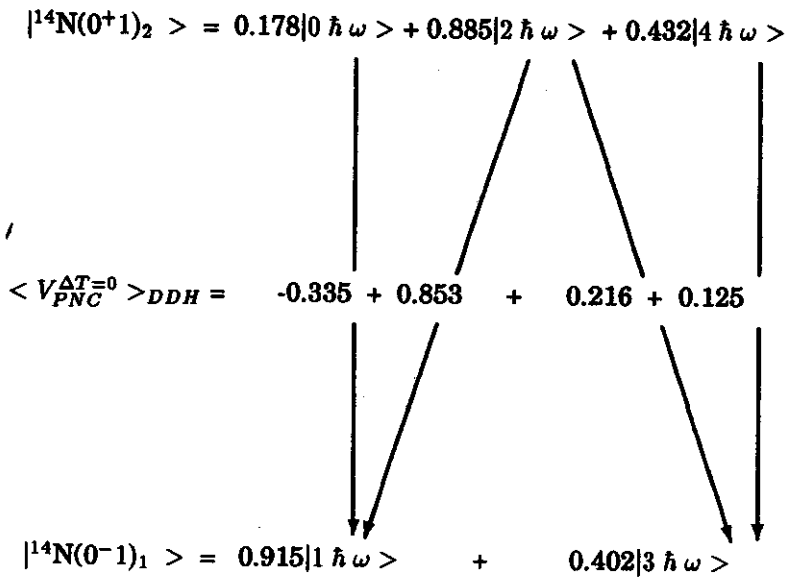

Figure 1: Decomposition of the PNC matrix element into the contributions coming from different $n\hbar\omega$ components of the wave functions. The calculation is that of model *c* and the DDH weak-coupling constants have been used. Units are eV.

a. Strahlenzentrum der Justus-Liebig-Universität, D-35392 Giessen, Germany.
b. Brookhaven National Laboratory, Upton, New York 11973.

References

1. E.G. Adelberger and W.C. Haxton, Ann. Rev. Nucl. Part. Sci. 35, 501 (1985).
2. N. Kniest, M. Horoi, O. Dumitrescu and G. Clausnitzer, Phys. Rev. C44, 491 (1991).
3. E.G. Adelberger, P. Hoodbhoy and B.A. Brown, Phys. Rev. C30, 456 (1984); Phys. Rev. C33, 1946 (1986).
4. V.J. Zeps et al., A.I.P. Conf. Proc. 176, 1098 (1989).
5. E.K. Warburton and B.A. Brown, Phys. Rev. C46, 923 (1992).

SCALING LAW IN CLUSTER DECAY

Mihai Horoi, B. Alex Brown and Aurel Sandulescu[a]

It was recently shown [1] that the known alpha decay $logT_{1/2}$ of the even-even nuclei with Z≥76 stay on the universal line

$$logT_{1/2} = 9.54\frac{Z_d^{0.6}}{\sqrt{Q_\alpha}} - 51.37\,, \tag{1}$$

with a rms deviation of 0.33. It is of interest to know if similar scaling law(s) exist(s) for cluster decay. We look to even-even parents and clusters with the hope that the structure effects are limited and only the collective dynamics dominates the process. Eq. (1) has been compared to what one obtains from the classical Gamow formula assuming a square well plus a Coulomb potential for the radial dynamics

$$logT_{1/2} = C_o + 2\cdot log2\cdot\frac{Z_dZ_c}{\sqrt{Q_\alpha}}e^2\sqrt{2\mu/\hbar^2}[arccos(x) - x\sqrt{1-x^2}]\,, \tag{2}$$

where

$$x = \sqrt{\frac{Q_c(R_c+R_d)}{Z_cZ_de^2}} \tag{3}$$

and where Q_c is the cluster decay Q-value and the R are the equivalent hard-sphere charge radii and $C_o = log(ln2/\omega P_o)$. The above analysis indicates that the scaling variable is

$$S = \frac{(Z_cZ_d)^{0.6}}{\sqrt{Q_c}}\,. \tag{4}$$

We have looked for the behavior of the known experimental data on cluster decay (see e.g Table 1 from Ref. [2]) as a function of this cluster scaling variable. The data are presented in Fig. 1. This analysis indicates a scaling law for the cluster decay (alpha included) similar to Eq. (1)

$$logT_{1/2} = C_1(S-7) + C_2\,. \tag{5}$$

It is interesting to examine if there are some correlations between the C_1 and C_2 coefficients corresponding to different cluster decays. Guided by Eq. (2) and by the fact that some models [3,4] indicate a $\sqrt{\mu}$ dependence of the prescission part, we have plotted in Fig. 2 the C_1 and C_2 coefficients as a function of $\sqrt{\mu}$. One can clearly see a linear dependence on $\sqrt{\mu}$ of these coefficients (the fitted lines are given by $C_1 = 6.3\sqrt{\mu} - 6.2$, $C_2 = 9.8\sqrt{\mu} - 26.9$).

The above analysis indicates a *model independent* law for the whole body of cluster decay data of the following form:

$$logT_{1/2} = (a_1\mu^x + b_1)\left[(Z_cZ_d)^y/\sqrt{Q} - 7\right] + (a_2\mu^x + b_2)\,. \tag{6}$$

A fit of the 119 alpha decays [1] and 11 cluster decays [2] from even-even parents has been done. Besides the 8 cluster data belonging to the specific sets described above (see Fig. 1), 3 "single" cluster data have been taken into the fit: ^{20}O from ^{228}Th ($logT^{exp}_{1/2}$=20.9), ^{32}Si from ^{238}Pu ($logT^{exp}_{1/2}$=25.3) and ^{34}Si from ^{242}Cm ($logT^{exp}_{1/2}$=23.2). The fit result gives $a_1 = 9.1$, $b_1 = -10.2$, $a_2 = 7.39$, $b_2 = -23.2$, $x = 0.416$ and $y = 0.613$ with a 0.34 rms deviation of $logT_{1/2}$. Considering the important parameter x, a range of values from 0.4 to 0.6 can be obtained depending upon the various subsets of data used in the fit. A 0.58 rms is extracted for the heavy clusters only, which represents a fairly good description of the data if one has in mind that the largest deviation comes from ^{34}Si ($logT_{1/2}$=24.45 as compared with the 23.2 experimental value).

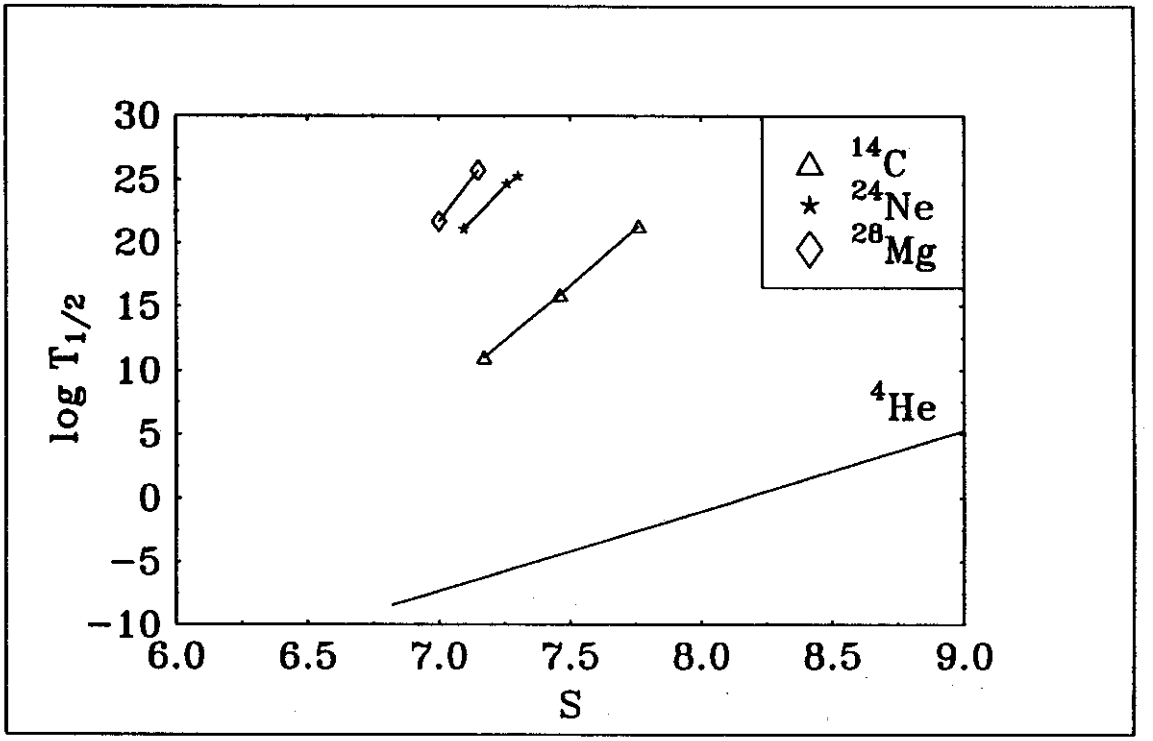

Figure 1. Experimental data for $logT_{1/2}$ (sec) of the cluster decay of even-even parents as functions of the scaling variable S (Eq. (4)). The line noted by ^{4}He is given by Eq. (1) which represents the best linear fit to the experimental data. Other lines are drawn to guide the eye.

Eq. (6) represents the first *model independent* description of all known cluster decay data. The parameters a_1, b_1, a_2, b_2, x and y contain information on the dynamics of the decay. The actual theoretical models describing the cluster decay data are rather crude. Often their parameters loose their physical meaning, as for example the unphysically small radii or the use of a zero-point motion energy even in the asymptotic region [3]. In our approach we have emphasized the most important variables (S, $\sqrt{\mu}$) scaling the experimental data. We expect this new approach to be an important step toward a theoretical description of the cluster decay.

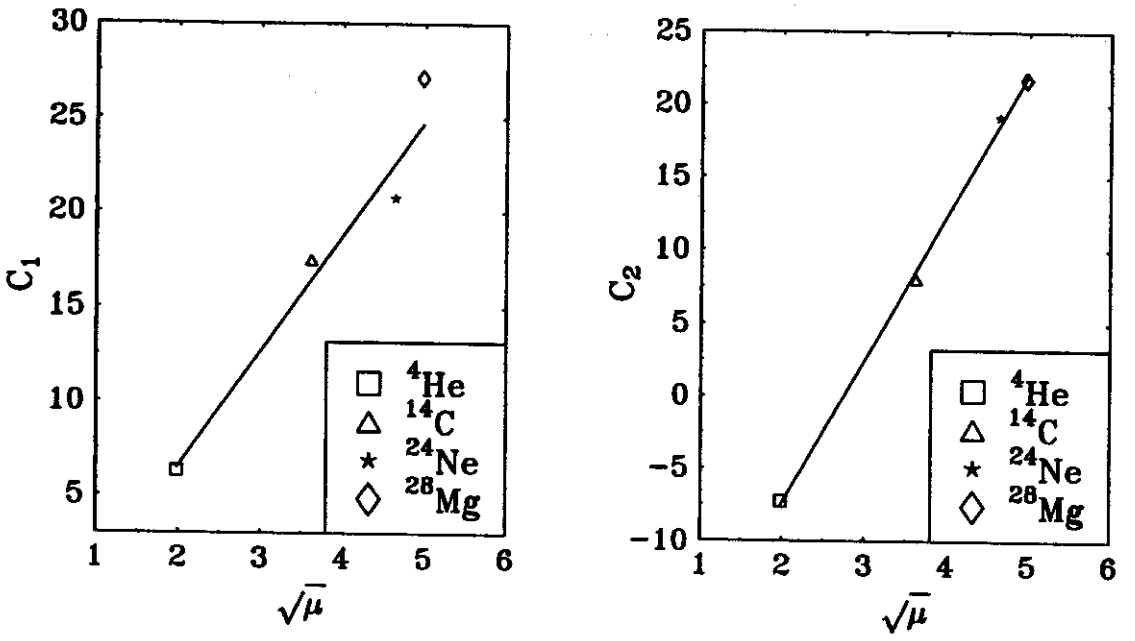

Figure 2. C_1 and C_2 coefficients entering Eq. (5) as function of $\sqrt{\mu}$. Lines represent the best linear fit.

a. Institute of Atomic Physics, Bucharest, Romania

References

1. B. A. Brown, Phys. Rev. C46 , 811(1992).
2. A. Sandulescu and W. Greiner, Rep. Prog. Phys. 55, 1423(1992).
3. D. N. Poenaru, W. Greiner, K. Depta, M. Ivascu, D. Mazilu and A. Sandulescu, At. Data Nucl. Data Tables 34, 423(1986).
4. Y.-J. Shi and W. J. Swiatecki, Phys. Rev. Lett. 54, 300(1985); Nucl. Phys. A438, 450(1985).

CAN ONE UNDERSTAND THE RESULTS OF THE PNC EXPERIMENTS IN A=18-21 NUCLEI?

Mihai Horoi and B. Alex Brown

The experimental PNC results in ^{18}F, ^{19}F, ^{21}Ne and their theoretical analysis[1] show a discrepancy. Namely, if one interprets the small limit of the experimentally extracted PNC matrix element (< 0.029 eV) for ^{21}Ne as a destructive interference between the isoscalar and the isovector contributions, then it is difficult to understand why the isovector contribution in ^{18}F is so small (< 0.09 eV) while the isoscalar + isovector contribution in ^{19}F is relatively large (0.40 ± 0.1 eV). In order to understand the origin of this discrepancy a new comparison of the calculated PNC matrix elements has been made. Previous nuclear structure calculations of the PNC matrix elements have been carried out (see Table 6 from Ref. 1) using $(0+1+2)\hbar\omega$ configurations for ^{18}F and $(0+1)\hbar\omega$ for ^{19}F and ^{21}Ne. Table 1 presents results for ^{18}F obtained in the smaller ZBM model space[3], but including up to $4\hbar\omega$ configurations. One can see that the contributions from 3 and 4 $\hbar\omega$ configurations are significant.

Table 1. Partial contributions to PNC matrix elements (eV units). Here and in the following calculations DDH weak couplings[1] are used.

Nucleus	Interaction[3]	ΔT	$0\hbar\omega$ - $1\hbar\omega$	$2\hbar\omega$ - $1\hbar\omega$	$2\hbar\omega$ - $3\hbar\omega$	$4\hbar\omega$ - $3\hbar\omega$
^{18}F	F-psd	1	1.045	-0.815	0.549	-0.187
	Z-psd	1	1.119	-0.778	0.462	-0.148
	ZBMO	1	1.297	-0.669	0.430	-0.118

We performed also a large scale shell model calculation for ^{18}F using the Warburton-Brown interaction[4]: the first 4 major shells describe the shell model basis and up to $3\hbar\omega$ configurations have been included for the first time. Results presented in Fig.1 confirm the necessity to include higher $\hbar\omega$ configurations. Guided by these results we reexamine the ZBM $(0+1+2+3+4)\hbar\omega$ calculations to see if the above mentioned discrepancy can be resolved.

Figure 1. Wave functions amplitudes and partial contributions to the PNC matrix element (eV) in a $(0+1+2+3)\hbar\omega$ calculation.

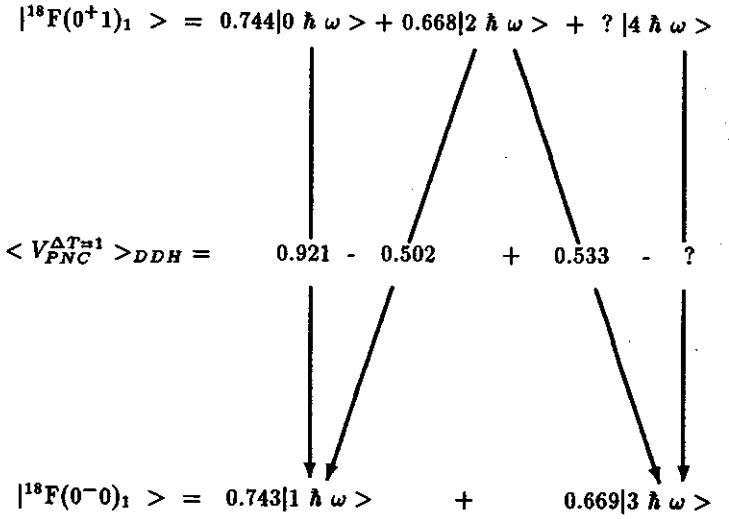

Table 2 presents different contributions to the PNC matrix element for ^{21}Ne. One can see that the isovector (IV) part is rather stable while the is isoscalar (IS) part fluctuates. These results are in contradiction with the usual interpretation[1] of the smallness of the PNC matrix element for ^{21}Ne.

Table 2. Isoscalar and isovector contribution to the PNC matrix element (eV) in ^{21}Ne.

Nucleus	Interaction	IS	IV	Total
^{21}Ne	F-psd	-0.113	0.556	0.442
	Z-psd	0.071	0.359	0.430
	ZBMO	-0.010	0.339	0.329

To reproduce the experimental results one can introduce weighting factors

$$< V_{PNC} >= \alpha_{IS}\beta_{IS} < V_{PNC}^{DDH}(IS) >_{ZBM} + \alpha_{IV}\beta_{IV} < V_{PNC}^{DDH}(IV) >_{ZBM} \quad (1)$$

The β factors take into account the renormalization effects due to the orbitals missing in the ZBM model space. A value of $\beta_{IV} = 0.59$ can be obtained from the comparison with the $^{18}N \rightarrow {}^{18}F$ first forbidden beta decay result[1]. A value of $\beta_{IS} = 0.48$ was estimated from a comparison with a recent $(0+1+2+3+4)\hbar\omega$ calculation[5] in ^{14}N. The α factors represent the ratio of the actual weak coupling constants to the DDH best values. An $(\alpha_{IS}, \alpha_{IV})$ plot, similar to that in Fig. 11 from Ref. 2 is presented in Fig. 2; it shows an overlapping region for the ^{18}F, ^{19}F and ^{21}Ne data. The $(\alpha_{IS}, \alpha_{IV})$ values in the overlapping region are in the range (0.6-1.2, 0.07-0.26).

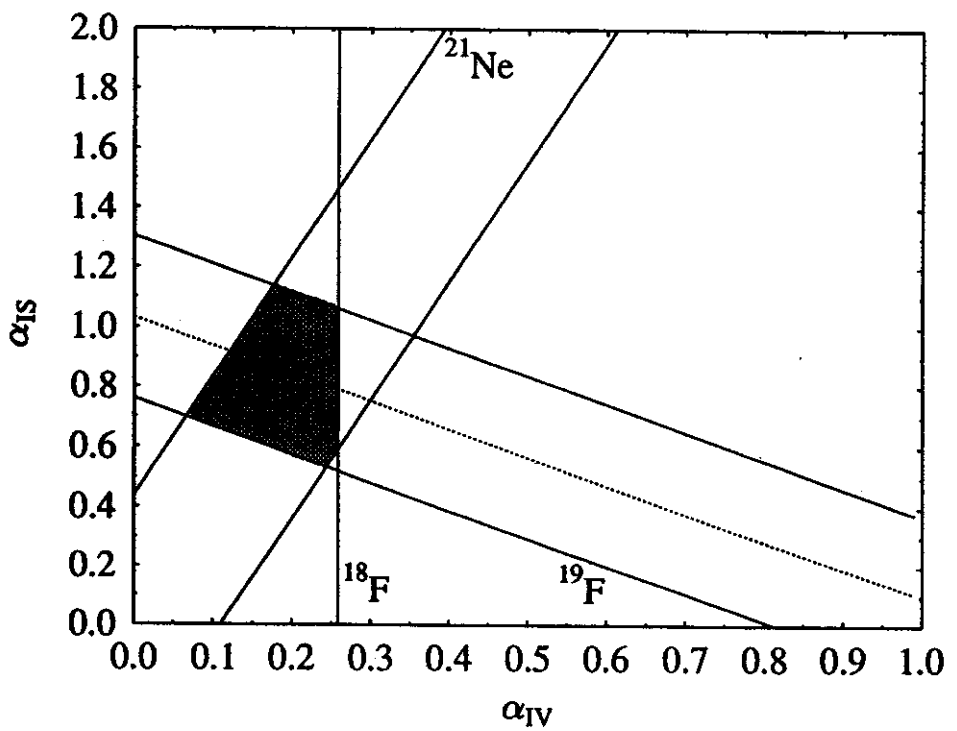

Figure 2. The $(\alpha_{IS}, \alpha_{IV})$ plot described in the text.

In conclusion, we have shown the necessity of including up to $4\hbar\omega$ configurations in the calculations of the PNC matrix elements of the light nuclei and have shown that the normalized ZBM calculations are not in contradiction with the experimental data.

References

1. E.G. Adelberger and W.C. Haxton, *Ann. Rev. Nucl. Part. Sci.* 35:501(1985).
2. S.A. Page et al., *Phys. Rev.* C 35:1119(1987).
3. B.A. Brown et al., *MSUNSCL Report*, 524 (1988).
4. E.K. Warburton and B.A. Brown, *Phys. Rev.* C46:923(1992).
5. M. Horoi, G. Clausnitzer, B.A. Brown and E.K. Warburton, Phys. Rev. C

CHAOS IN NUCLEI AND DYNAMICS OF GIANT RESONANCES

V.G.Zelevinsky

Chaotic dynamics became recently a hot issue. Whereas classical chaos, especially for a small number of degrees of freedom, is well understood, quantum chaos is still a virgin land. In spite of lack of a rigorous mathematical definition of quantum chaos (many physicists prefer to speak about classical signatures of quantum chaos only), quite a few interesting results show that the idea can be productive in understanding physics of actual many-body quantum systems.

Near the ground state, a many-body system can be described in terms of almost independent elementary excitations (quasiparticles) moving in a self-consistent mean field. As excitation energy and level density increase, the residual interaction gets more and more important. Stationary states become extremely complicated combinations of many elementary excitations. Individual level correlations and fluctuations display generic features of quantum chaos similar to the Gaussian Orthogonal Ensemble (GOE) of random matrices. Presumably, more physical information can be learnt from the analysis of wave functions and matrix elements.

The important feature of many-body chaos [1] is coexistence of regular motion (mean field and collective modes) with chaotic incoherent dynamics. In some sense, the mean field itself is generated by the averaging out the random collision-like processes [2]. The interplay between collective and chaotic dynamics has profound influence onto giant resonances (GR). Recent data [3] show that the damping width of GR saturates as a function of temperature at $T \leq 2MeV$. This can be understood from the very general viewpoint as a result of complete mixing of stationary states (*stochastic limit* of dynamics [4]).

In the stochastic limit, matrix elements of "simple" (one- or two-body) operators between complicated states, as well as between a complicated and a simple state, scale $\sim 1/\sqrt{N}$ where N characterizes the localization length of complicated states in the "natural" mean field representation. The idea of N-scaling was successful in explaining remarkable enhancement of weak interaction in compound states [5].

Consider a GR as a simple state embedded into a sea of states with a very complicated structure. The residual interaction mixes the GR with doorway states of the next degree of complexity and so on. In the stochastic limit this evolution leads to the spreading width $\Gamma^{\downarrow}$ which ceases to grow beyond the value of the order of typical matrix elements of the residual interaction between simple states. Using as a model the standard expression for the spreading width,

$$\Gamma^{\downarrow} = 2\pi \frac{\langle V^2 \rangle}{D}, \tag{1}$$

we see the mechanism of the saturation: both the average mixing matrix element $\langle V^2 \rangle$ of coupling between the GR and (already mixed) background states, and the level spacing D are decreasing $\sim N^{-1}$ with temperature increasing.

The saturation phenomenon was clearly seen and discussed [6][7] in similar way also for isobaric analog states where the spreading width, related in this case to the isospin purity, manifests remarkably small variations throughout the periodic table regardless of excitation energy, spin and isospin of the state.

We see that in the observables like the spreading width (1) the exponentially growing quantitites associated with the underlying level density are eliminated. The saturation regime is expected to be violated at higher temperatures where the escape width and continuum effects become dominant.

References

1. V.G.Zelevinsky. Nucl. Phys. A553 (1993) 125c.
2. V.G.Zelevinsky. Nucl. Phys. A555 (1993) 109.
3. J.J.Gaardhøje. Ann. Rev. Nucl. Part. Sci. 42 (1992) 483,
4. V.G.Zelevinsky, P.F.Bortignon and R.A.Broglia. Preprint NBI-93-45.
5. V.V.Flambaum and O.P.Sushkov. Nucl. Phys. A412 (1984) 13.
6. H.L.Harney, A.Richter and H.A.Weidenmüller. Rev. Mod. Phys. 58 (1986) 607.
7. V.G.Zelevinsky and P. von Brentano. Nucl. Phys. A529 (1991) 141.

CHAOS AND ORDER IN THE SHELL MODEL EIGENVECTORS

Vladimir Zelevinsky, Mihai Horoi and B. Alex Brown

Quantum chaos in many-body systems was studied mostly from the viewpoint of level statistics which displays a clear relation to the notion of classical chaos. Presumably much more information could be obtained from an analysis of the wave functions and transition amplitudes. To perform such an analysis and to check various hypotheses concerning complicated quantum dynamics, one needs a rich set of data which would allow one to make statistically reliable conclusions. Realistic nuclear shell model calculations are one of the most promising candidates for studying this largely unknown structure of quantum chaotic states.

The behavior of the basis-state amplitudes of the shell model eigenvectors produced in the $J-T$ scheme is studied for 12 particles in the *sd* shell. Our model hamiltonian describing a many-body system of valence particles within a major shell contains a one-body part, which is mainly due to an existing core (e.g. ^{16}O for the *sd* shell) and a two-body antisymmetrized interaction of the valence particles

$$H = \sum \epsilon_\mu a^\dagger_\mu a_\mu + \frac{1}{4}\sum V_{\mu\nu\lambda\rho} a^\dagger_\mu a^\dagger_\nu a_\lambda a_\rho \ . \tag{1}$$

The $J-T$ projected states $\mid k\rangle$ are used to build the matrix of the many-body hamiltonian, $H_{kk'} = \langle JT;\ k \mid H \mid JT;\ k'\rangle$, which is eventually diagonalized producing the eigenvalues E_α and the eigenvectors

$$\mid JT;\ \alpha\rangle = \sum_k C^\alpha_k \mid JT;\ k\rangle. \tag{2}$$

They represent the object of our investigation.

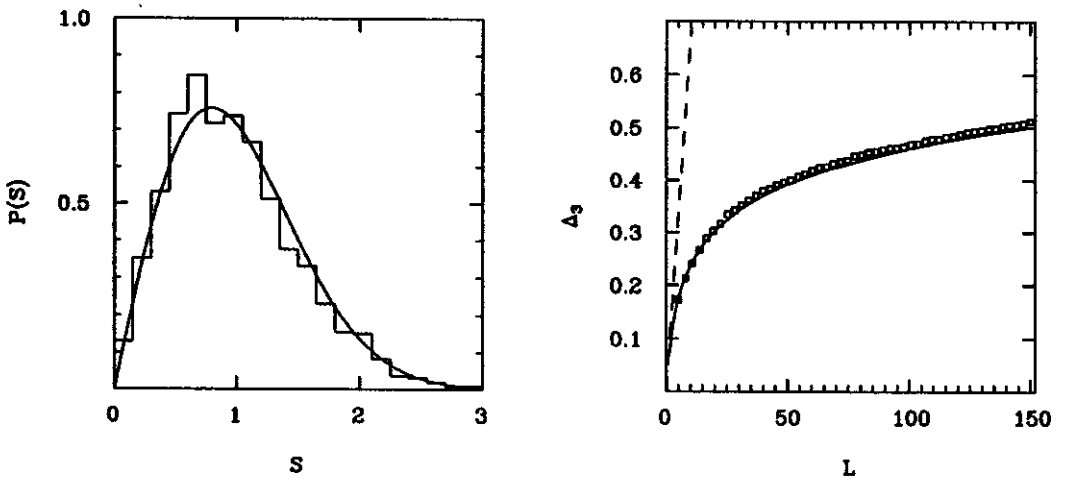

Figure 1: Unfolded distribution of the nearest neighbor spacing (left) and the rigidity of the spectrum, $\bar{\Delta}_3$, (right).

The matrix dimension for the $J^\pi T = 2^+0$ states is 3273. Fig. 1 shows the standard quantities which define the chaoticity of a quantum system [1], the unfolded distribution of the nearest neighbor spacing $P(s)$ and the spectral rigidity $\bar{\Delta}_3$. for this class of states. The solid lines in both parts of the figure describe the

random matrix results for the Gaussian Orthogonal Ensemble. The dashed line on the right corresponds to the Poisson level distribution which is characteristic of an ordered system. The closeness of $\bar{\Delta}_3$ to the random matrix results even for very large values of L is remarkable. Previous to this study the largest value of L considered was 40 [2]. Thus, the level statistics manifest typical chaotic behavior.

We next look to other quantities which could reveal in more detail how close to chaoticity we are.

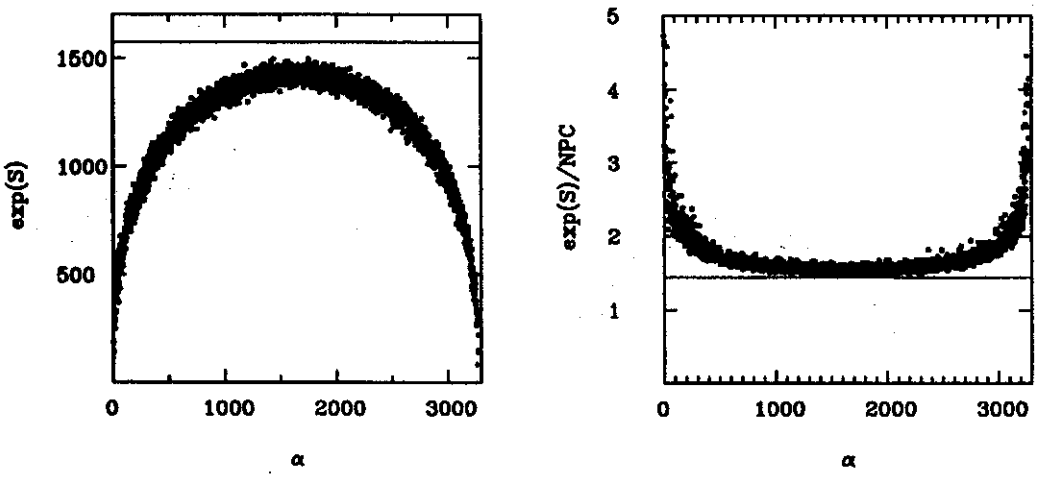

Figure 2: Exponential of entropy (left) and the ratio of this quantity to the Number of Principal Components (right) as functions of the eigenvector number (order by the eigenvalues).

The appropriate quantities to measure the degree of complexity of a given eigenstate (2) with respect to the original shell model basis are, for instance, the informational entropy [3],

$$S^\alpha = -\sum_k |\, C_k^\alpha \,|^2 \ln |\, C_k^\alpha \,|^2, \tag{3}$$

or the moments of the distribution of amplitudes C_k^α. The second moment determines the number of principal components (NPC) of an eigenvector $|\alpha\rangle$,

$$(NPC)^\alpha = \left(\sum_k |\, C_k^\alpha \,|^4 \right)^{-1}. \tag{4}$$

The random matrix results for these two quantities averaged over the GOE are $\ln(0.48N)$ and $N/3$ respectively, where N is the dimension of the model space. The left part of Fig. 2 presents the $\exp S^\alpha$ for the 2^+0 states. On the x-axis are the eigenstates numbered in order of their energies. This simple "numbered" scale is equivalent to the natural "unfolding" procedure described for example by Brody *et al.* "Unfolding" is introduced to separate local correlations and fluctuations from the global spectral properties. The solid line represents the GOE result ($0.48N$). One observes a semicircle-type behavior and a 12% deviation from the GOE even for the maximum entropy in the middle of the spectrum. The NPC has a similar behavior. However, for the ratio of these quantities one obtains the results in the right part of

Fig. 2. The solid line is the universal (N-independent) random matrix result equal to 1.44. The flattened region indicates that the chaotic dynamics, even if not complete, extends far beyond the region nearby the maximum of the informational entropy (compare with the left side of Fig. 2). The "unfolding" reveals the presence of "local" chaos: in a given small energy range, the eigenstates are characterized by a typical delocalization length $N^\alpha < N$ and by Gaussian distribution of the amplitudes C_k^α with zero mean value and variance $(N^\alpha)^{-1}$. This length cancels in the ratio $\exp(S^\alpha)/(NPC)^\alpha$ for the majority of states in the middle of the spectrum. The flatness of this ratio, as compared to strong α-dependence of $\exp(S^\alpha)$ and $(NPC)^\alpha$ separately, indicates the existence of the local chaotic properties scaling with N^α.

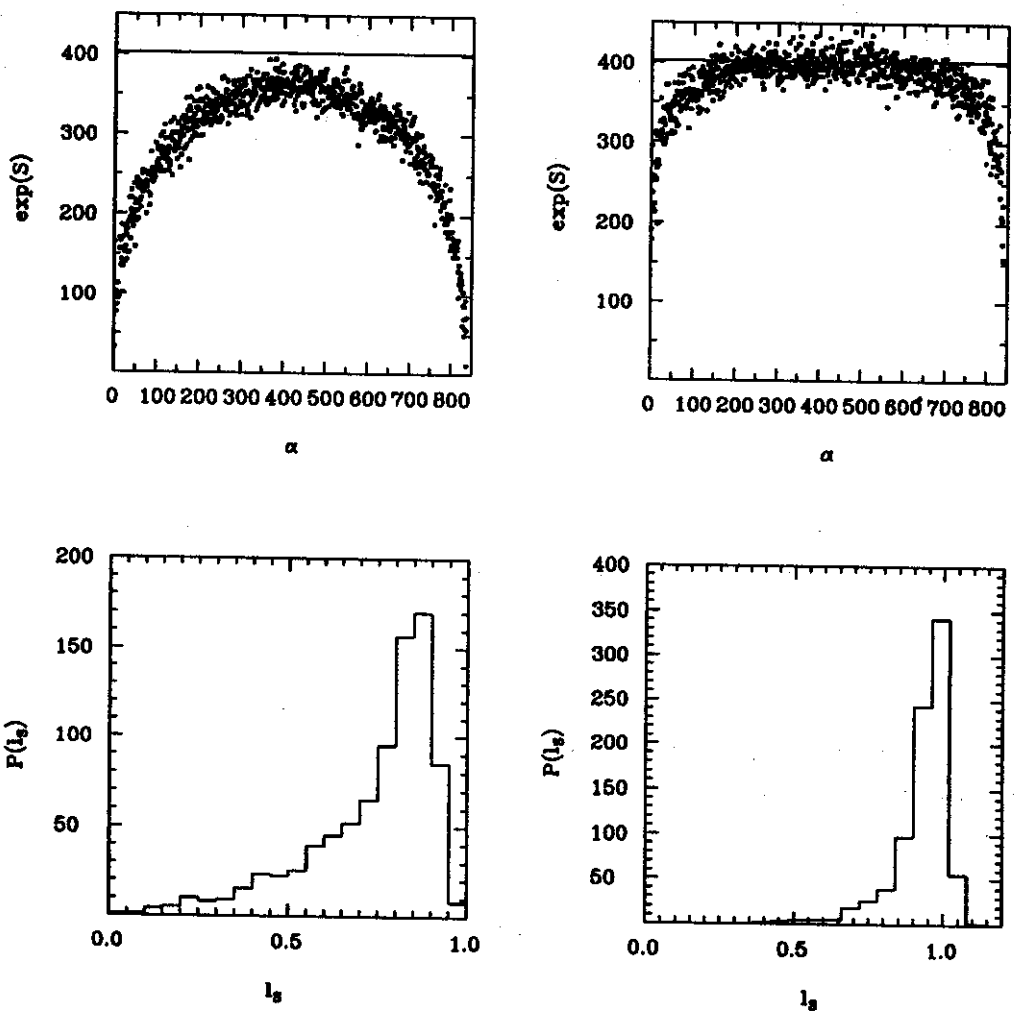

Figure 3: The exp(S) and the distribution of $l_S = \exp(S)/0.48N$ for the 0^+0 states (further explanations in the text).

It is interesting to study the role of single-particle energies (see eq. (1)) for the chaotic behavior of the amplitudes. The upper part of Fig. 3 shows the $\exp(S)$ quantity for the 0^+0 states (JT dimension 839) when the normal Wildenthal hamiltonian [4] is used (left) and for the same hamiltonian but with all single particle energies, ϵ_μ in eq. (1), zero (right). In the last case the GOE limit (solid line) is attained and the chaotic regime extends over a larger part of the spectrum. To further quantify these effects, we look to the

distribution $P(l_S)$ of the $l_S^\alpha = \exp(S^\alpha)/0.48N$. One can interprete l_S^α as a localization length N^α/N. It is expected to be shaped around $l_S = 1$ in the chaotic limit. Fig. 3 (lower left panel) presents the results for the values of l_S calculated for the normal hamiltonian and shown on the upper left panel. Here the limit of $l_S = 1$ is basically not reached. On the other hand, for degenerate single-particle orbitals (upper and lower panels on the right side) the full chaotic limit is reached. This is related to the fact that the mean field tends to smooth out the chaotic aspects of many-body dynamics [5].

In conclusion, we have studied the chaotic properties of a many-body quantum system which consists of 12 valence particles interacting in the *sd*-shell. We have shown that standard quantities like nearest neighbor spacing distribution or spectral rigidity are not sensitive enough to show deviations from the random matrix results. The informational entropy or moments of the $\mid C_k^\alpha \mid^2$ distribution like (NPC) are much more suited to reveal these details. Arguments are given in favor of local chaos characterized by Gaussian distribution of the components of the wave functions with the variance related to the localization length. Finally, we have shown that the effect of the core (given by the single-particle energies) diminishes the maximal degree of chaoticity which can be obtained when the system consists of interacting valence particles only.

We point out that our signatures of complexity, l_S and (NPC), are basis-dependent. Nevertheless, it is remarkable that the shell model basis we have chosen sheds a detailed light on the global and local chaotic properties of the wave functions in the many-body system with strong interaction.

References

1. T.A. Brody et al., Rev. Mod. Phys. 53, 385(1981).
2. P. Arve, Phys. Rev. C44, 6920(1991).
3. F.M. Izrailev, Phys. Rep. 196, 299(1990).
4. B.A. Brown et al., OXBASH-code, MSUNSCL report 1988.
5. V.G. Zelevinsky, Nucl. Phys. A555, 109(1993).

TRUNCATION METHOD FOR THE SHELL MODEL CALCULATION IN ONE MAJOR SHELL

Mihai Horoi, B. Alex Brown and Vladimir Zelevinsky

In this work we outline a quantitative method to truncate the huge nuclear shell model spaces to manageable sizes. To achieve this we show that the basis states whose unperturbed energies (the diagonal matrix element of the hamiltonian) are far away from the lowest one have a small contribution to the structure of the ground states and the few low lying states. This statement can be quantified due to an interesting property of the squared amplitudes of the basis states (denoted by the index k), $\mid C_k^\alpha \mid^2$, as a function of the eigenvalues, E_α. One can show that their distribution is quite close to a Gaussian, with mean values (centroids) exactly the diagonal matrix elements of the hamiltonian

$$\bar{E}_k \equiv \sum_\alpha \mid C_k^\alpha \mid^2 E_\alpha = H_{k,k} \tag{1}$$

and their widths given by

$$\sigma_k \equiv \sqrt{\sum_\alpha \mid C_k^\alpha \mid^2 E_\alpha^2 - \bar{E}_k^2} = \sqrt{\sum_{k' \neq k} H_{k',k}^2} \tag{2}$$

The small squares in Fig. 1 represent these quantities for the case of 12 particles in the sd shell with $J^\pi T = 0^+0$. The Wildenthal interaction has been used for this plot. We have checked different interactions and we have carried out calculations in the fp shell also, but the results are qualitatively the same. To obtain the points no diagonalization is necessary but only the knowledge of the hamiltonian matrix.

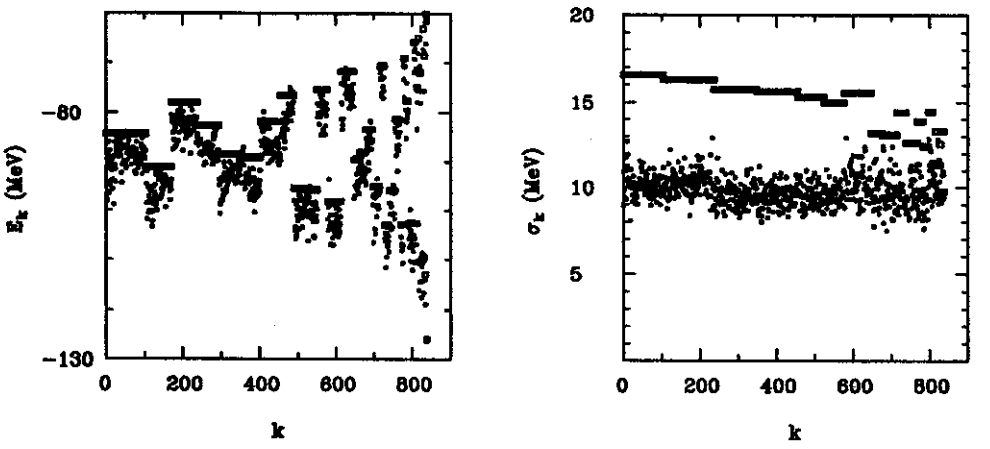

Figure 1: Energy centroids and σ widths of the basis states coefficients distribution (see Eqs. (1)-(2))

Due to the empirical fact that σ is constant for all basis states we can, for example, consider only those basis states whose centroids are lower than $H_{cutoff} = (\bar{E}_k)_{min} + 3\bar{\sigma}$, where $\bar{\sigma}$ is an average value for σ_k.

One would like also to avoid the construction of the huge hamiltonian matrix. A useful procedure is to use some average values for the quantities in Eqs. (1)-(2). One simple way to proceed is to use the average values given by French and Ratcliff [1]. They are presented in Fig. 1 by the big squares. They are constant within every partition of particles in the single particle levels. The average values slightly overestimate the exact values due to the fact that they are derived for the m-scheme whereas the physical states we work with are projected onto good angular momentum and isospin. However, the m-scheme estimate is good enough for our purpose.

Our method consists in retaining only those partitions whose average centroids (calculated with the approximate formulae [1]) are smaller than H_{cutoff}. The method has the advantage that one can include step by step new partitions in the order of their centroids. We have tested the method in the sd shell where we know the exact results. In Fig. 2 we show the results for the lowest 0^+1 states in the case of 10 particles in the sd shell. The left part shows the eigenvalues of the two low lying states as a function of dimension of the truncated space. The dimension of the full space is 1132. The filled circles (to the right) are the exact values. One can see that with relatively truncated spaces one can approach the exact eigenvalues. To have an another measure of the precision of the method we plotted in the right part of Fig. 2 the overlaps of the approximate ground state wave function with the exact ground state wave function (full line). One can see that with less than 30% of the full dimension one can obtain more than 90% overlaps. The dashed line represents the "optimal" truncation in the sense that we retained only those basis states whose exact amplitudes are the highest. One can see that our simple truncation procedure is near to the "optimal" one.

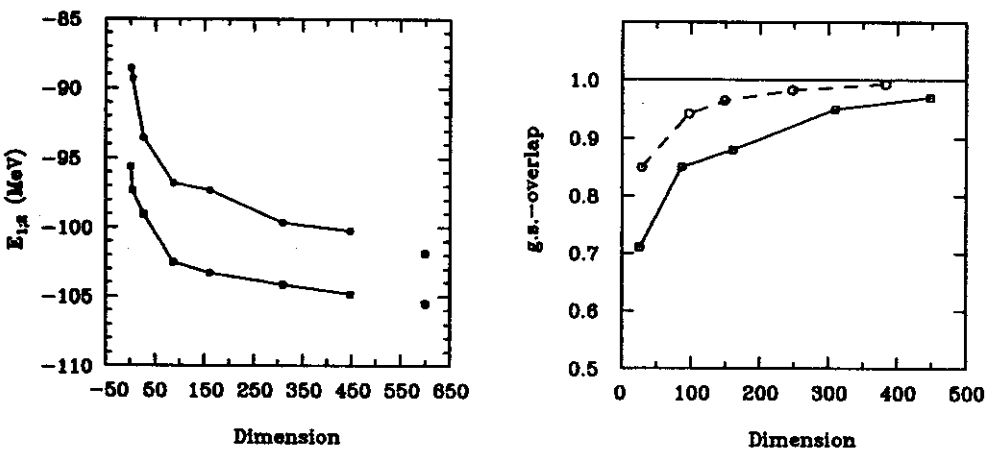

Figure 2: Energies of the two low lying states versus the dimension of the truncated space (left); overlaps of the truncated space wave functions with the exact ones (right).

Our investigations in the sd shell (maximum JT dimension of the order of few thousands) show that using this method one can reduce the dimension of the hamiltonian matrices by a factor of 3. Going to larger model spaces one can expect that this factor to be even higher. This is to be expected if simple

shell model configurations (e.g. those with the lowest E_k in the left side of Fig. 1) represent a reasonable approximation to the exact ground state wave function. In this last case some of the basis states amplitudes will be of the order of ten(s) of percents and the number of the very small (discardable) amplitudes will increase (due to the normalization). To have an impression about this effect we calculated the low lying states of ^{54}Fe (14 particles in the fp shell, the 0^+1 states and Brown-Richter interaction [2]) using our truncation method. The dimensions of the problem make the traditional calculations unmanageable even with the next generation of computers: 2229178 JT dimension and 345400274 m-scheme dimension. The results of our truncation method are presented in Fig. 3. We don't have exact results to compare, but we can refer to the result of a recent Monte Carlo calculation [3] (the filled circles with errors bars).

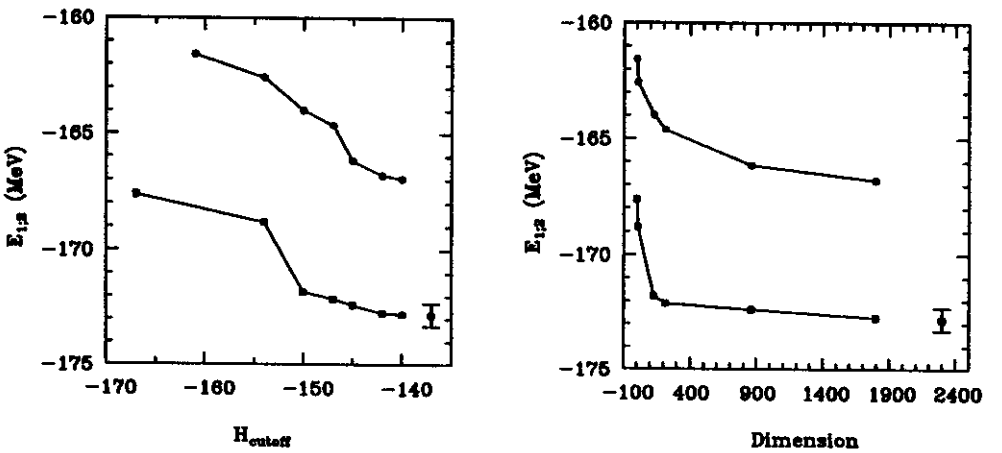

Figure 3: Energies of the first two low lying states of ^{54}Fe as a function of truncation diagonal matrix element (left) and versus the dimension of the truncated space (right). The filled circles with the error bars are the result of a recent Monte Carlo calculation [3].

The comparison is encouraging and we believe that we should be able to calculate energies to within less than one MeV accuracy for the ground states and low-lying exited states for even larger model spaces. One also note that the present method might be used as a criteria for an importance sampling mechanism for any kind of Monte Carlo methods, like the "stochastic diagonalization" [4], due to its ability to identify the most important configuration contributing to the structure of the low-lying state. Its may also be applied to more general calculations such as those for atoms, molecules or atomic clusters.

References

1. J.B. French and K.F. Ratcliff, Phys. Rev. C3, 94(1971).
2. W.A. Richter et al., Nucl. Phys. A532, 325(1991).
3. Y. Alhassid et al., Phys. Rev. Lett. 72, 613(1994).
4. H. De Raedt and M. Frick, Phys. Rep. 231, 107(1993).

WIDTHS OF MULTIPLE GIANT RESONANCES

C.A.Bertulani, C.H.Lewenkopf and V.G.Zelevinsky

Recent experiments [1] on excitation of multiple (double and even triple) dipole giant resonances (GR) indicate relatively narrow widths: for double resonances the width Γ_2 is about 1.5 of the width Γ_1 of single GR. This width is associated with the damping of the collective mode the contribution of the escape width being rather small. Here, contrary to the usual sound attenuation, we can study the damping of a state with a definite number of quanta in the quantum limit of low temperature, $T \ll \hbar\omega$, which is not accessible in macroscopic Fermi liquids.

The excitation of multiple GR in heavy ion collisions and their damping were discussed in [2]. Since the dominating excitation mechanism is sequential one and the anharmonic effects are weak, the strength function of the double GR can be found by the convolution of the strength functions for single resonances,

$$S_2(E) = \int dE_1 dE_2 \delta(E - E_1 - E_2) S_1(E_1) S_1(E_2). \tag{1}$$

For Breit-Wigner (or Lorentzian) distribution S_1, it would give the ratio of widths of the n-phonon and single GR $r_n = \Gamma_n/\Gamma_1 = n$. The same conclusion is obtained in specific models using the standard expression $\Gamma^{\downarrow} = 2\pi\langle V^2\rangle/D$ for the spreading width. If, according to the Brink-Axel hypothesis, phonons are created on top of each other, and they decay independently, the density of background states $1/D$ is always the same and the Bose-factor $\sqrt{n}$ in the matrix elements $\langle n-1|V|n\rangle$ leads to $r_n = n$.

For Gaussian distribution or any distribution with a finite second moment $\langle(\delta E)^2\rangle$ the variances add in quadratures which results in $r_n = \sqrt{n}$. It means that the wings of the strength function due to the coupling of GR to remote background states are crucial for the lineshape and r_n.

The problem was analyzed [3] from the viewpoint of quantum chaotic dynamics. In the stochastic limit the doorway states for the decay of the GR have their own spreading widths saturated on the level of the typical matrix elements Δ of the residual interaction between simple states. The background states located at a distance $\delta E > \Delta$ from the position of the collective GR are sterile since they do not carry the doorway strength. Meanwhile the standard expression for the spreading width assumes, among other approximations, the uniform coupling V to all complicated states uncorrelated to their position. In the stochastic limit matrix elements scale like $V \simeq v/\sqrt{N}$ with the localization length N of the complicated states. The standard model is valid if $v \ll \Delta$ in which case $\Gamma/\Delta \sim (v/\Delta)^2 \ll 1$. It implies the Breit-Wigner shape and $r_n = n$ (exponential in time independent decay of n phonons),

In the opposite situation of $v > \Delta$, the strength covers the region *linearly* increasing with v and therefore growing $\sim \sqrt{n}$ with the phonon number. Already at $v \simeq \Delta$ which is appropriate for the GR, the transition occurs from the Breit-Wigner shape to the shape with a finite $\langle(\delta E)^2\rangle$ and therefore from $r_n = n$ to $r_n = \sqrt{n}$. Actually, the central limit theorem very fast drives the lineshape [1] to the Gaussian one.

We made numerical simulations for the GR coupled to the background modeled by the random matrix ensemble (GOE). The matrix element $V(\epsilon)$ for the coupling between the GR at the origin and the background state at energy ϵ was supposed to be Gaussian distributed with the variance

$$\langle V^2(\epsilon)\rangle = V_0 \exp(-\epsilon^2/2\Delta^2). \tag{2}$$

Fig. 1 shows a clear transition from the standard results, $r_2 = 2$, when Δ exceeds the spreading width $\Gamma^{\downarrow}$ calculated according to the usual "golden rule", to $r_2 = \sqrt{2}$ at $\Delta \approx \Gamma^{\downarrow}$.

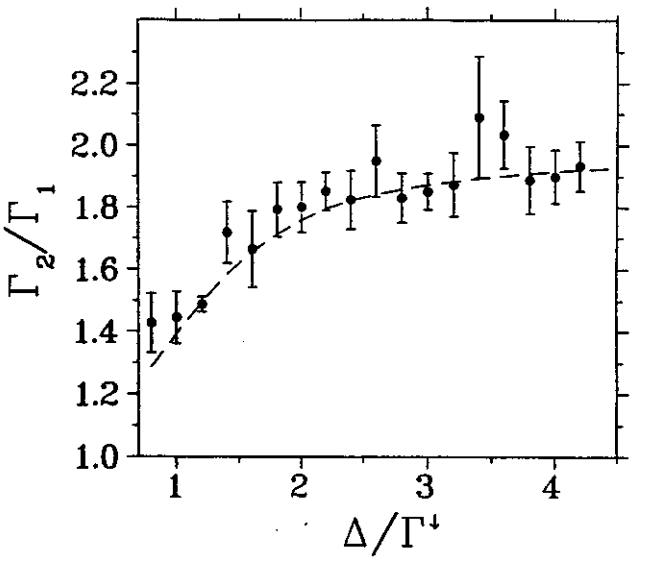

Figure 1: Double phonon - single phonon width ratio as a function of the parameter Δ, eq. (2), in units of the standard spreading width. Points stand for the numerical simulation (ensemble of 500 matrices 200×200); dashed line is the exact diagonalization for the picket fence background spectrum.

References

1. S.Mordechai *et al.* Phys. Rev. C41 (1990) 202; J.Ritman *et al.* Phys. Rev. Lett. 70 (1993) 533; R.Schmidt *et al.* Phys.Rev. Lett. 70 (1993) 1767; T.Aumann *et al.* Phys. rev. C47 (1993) 1728.
2. C.A.Bertulani and V.G.Zelevinsky. Phys. Rev. Lett. 71 (1993) 967; Nucl. Phys. A568 (1994) 931.
3. C.H.Lewenkopf and V.G.Zelevinsky. Nucl. Phys. A569 (1994) 183c.

TRANSITIONAL NUCLEI: SOFT MODE DYNAMICS

V.G. Zelevinsky

The problem of soft transitional nuclei is probably the oldest unsolved problem of nuclear structure. It was formulated by A.Bohr and B.Mottelson in the beginning of fifties. In spite of growing accumulation of experimental data and permanent theoretical efforts, we still do not understand the properties of low-lying states in dozens of nuclei with strong collective behavior but without well developed rotational bands.

The spectroscopic picture in such nuclei can be characterized by three main features.

- *Quadrupole symmetry.* Quantum numbers of almost all low energy levels are the same as predicted by a simple model of a quadrupole harmonic vibrator; intruder states are very rare. However, the quantitative predictions of the harmonic model are badly violated.

- *Collectivity.* There are strong collective $E2$ transitions up to rather high excitation energy (in many cases the complete spectroscopy is known up to 3-4 MeV and even higher). Enhancement factor with respect to single-particle estimates is typically 20-30.

- *Adiabaticity.* The energy spacing between levels linked by collective transitions (characteristic collective frequency ω) is small, $\tau \equiv \omega/2\bar{E} \ll 1$ where $2\bar{E}$ is a Cooper pair breaking energy (two-quasiparticle excitation).

It means that we have to deal with the large amplitude collective quadrupole motion, $Q \propto 1/\sqrt{\omega}$. In spite of absence of static deformation, a nucleus explores a variety of smoothly changing shapes. The popular interacting boson models (IBM) encounter serious difficulties in their attempts to describe soft nuclei. Apart from the modest quantitative agreement, they fail to explain the vibrational bands manifesting strong collectivity up to very high spins, much higher than allowed by simple conversion of all available bosons (their number in the IBM is fixed as a number of valence nucleon pairs) into quadrupole ones.

Earlier, the simple phenomenological model was suggested [1] based on strong quartic anharmonicity (term $\sim \beta^4$ in the classical Bohr-Mottelson quadrupole hamiltonian). In the physical domain of small ω, the quartic term dominates the dynamics similar to the vicinity of the second order phase transition in macroscopic systems. It restores the stability even after the phase transition when $\omega^2 < 0$.

This model gives a very good description of many transitional nuclei [1,3] As a rule, 15-20 levels are fitted with two or three parameters and relative transition probabilities between them require two additional parameters. The quartic anharmonicity ensures $O(5)$ symmetry which seems to be a good dynamical symmetry for soft nuclei. In some cases as the yrast band levels E_J in ^{100}Pd, the data show the exact symmetry predicted for a 5-dimensional quartic oscillator,

$$E_J = const(J+5)(J+7)^{1/3}. \tag{1}$$

The semiquantitative justification of the model was given in [4]. Straightforward estimates are based on the textbook properties of a nucleus as a self-sustained superfluid drop of Fermi liquid. In the vicinity of the instability point where the random phase approximation (RPA) predicts $\omega^2 \to 0$, the degree of collectivity Ω (enhancement factor of a collective transition amplitude $Q \simeq q\sqrt{\Omega/\tau}$ compared to a typical

single-particle amplitude q) and the adiabaticity parameter τ are interrelated according to

$$\Omega \simeq \sqrt{A}, \quad \tau \simeq A^{-1/6}, \quad \Omega\tau^3 \simeq 1. \tag{2}$$

The estimate (2) being in agreement with empirical trends allows one to discriminate the anharmonic terms beyond the RPA. The big difference in time scales for collective and single-particle motion makes high order anharmonicity weak. Only cubic, $\sim \beta^3 \cos 3\gamma$, and quartic terms are significant. In transitional nuclei, in addition, cubic terms are small due to the approximate particle-hole symmetry, similar to the Furry theorem in quantum electrodynamics. As a result, the dominating term is quartic one which leads to the gamma-unstable potential and $O(5)$ symmetry.

Thus, the derivation of consistent microscopic theory for soft nuclei is reduced to the calculation of parameters of the corresponding collective quadrupole hamiltonian with strong quartic anharmonicity. It should be done in a nonperturbative manner taking into account the coherent response of non-collective degrees of freedom to the large amplitude collective motion. To solve this problem, a special method was developed which can be helpful in various many-body applications.

Exact operator equations of motion for the density matrix $R \sim a^\dagger a$ are derived with the use of an actual many-body hamiltonian H,

$$i\dot{R} \equiv [R, H] = F\{R\}, \tag{3}$$

where the functional F contains terms linear and bilinear in R. On the other hand, we are looking for the collective hamiltonian $\mathcal{H}(\alpha, \pi)$ expressed in terms of collective coordinates α and conjugate momenta π. In the collective subspace the image $\mathcal{R}$ of the density matrix R is also a function of α and π satisfying the equations of motion determined by the supposed form of $\mathcal{H}$,

$$i\dot{\mathcal{R}} \equiv [\mathcal{R}, \mathcal{H}] = \mathcal{F}(\alpha, \pi). \tag{4}$$

The mapping of the dynamics onto the collective subspace is performed by the requirement of the saturation of dynamics within this subspace. It means that eqs. (3) and (4) should be consistent,

$$\mathcal{F}(\alpha, \pi) = F\{\mathcal{R}(\alpha, \pi)\}. \tag{5}$$

Analysis of this set of equations confirms the initial assumptions and estimates (2). The main driving force beneath the collective motion is redistribution of particles (the occupation numbers are now operators depending on collective amplitudes α^2 and π^2). In accordance with these dynamics, the superfluid gap is as well modulated by collective motion. The population dynamics can be described by a kinetic equation where exchange of energy between individual quasiparticles and the collective mode plays the role of the collision integral.

References

1. O.K.Vorov and V.G.Zelevinsky. Nucl. Phys. A439 (1985) 207.
2. O.K.Vorov and V.G.Zelevinsky. *In:* Modern Developments in Nuclear Physics, ed O.P.Sushkov (World Scientific, Singapore, 1988) p.281.
3. V.G.Zelevinsky. Soryushiron Kenkyu (Kyoto) 83 (1991) D176.
4. V.G.Zelevinsky. Int. J. Mod. Phys. E2 (1993) 273.

THRESHOLD FOR DISSIPATIVE FISSION

M. Thoennessen and G. F. Bertsch[a]

The standard Bohr-Wheeler statistical theory of fission fails to describe the fission process in hot nuclear systems. At high excitation energies the pre-fission neutron, charged particle and giant dipole resonance (GDR) γ-ray multiplicities exceed the predictions of the statistical model calculations, although the model works well at low excitation energy [1,2]. The enhanced pre-fission particle/γ-ray multiplicities can be attributed to a hindrance of fission as a consequence of either very large or very small dissipation of the collective motion. Thus, the excitation energy at which dissipation effects start to dominate is an important quantity in order to understand the origin and the excitation energy dependence of the dissipation mechanism.

We assembled data of the threshold energy E_{thresh} over a wide range of masses and fissilities from a wide variety of different experiments [3]. The threshold energy is defined as the excitation energy of the compound nucleus where calculations with the standard statistical model start to deviate from the pre-fission particle/γ-ray multiplicities. Thus E_{thresh} marks the upper energy limit where the statistical theory applies. Although a large set of excitation functions covering the relevant energy range exists already for quite some time, no detailed analysis of these data have been performed. We found a parameterization of E_{thresh} which is independent of the size of the system or the fissility. The ratio of the average threshold temperature over the average fission barrier turns out to be a constant independent of the system.

The threshold temperature T_{thresh} can be calculated from the threshold energy E_{thresh}: $T_{thresh} = \sqrt{(E_{thresh} - E_{rot})/a}$, where E_{rot} is the rotational energy and $a = A/9$ is the level-density parameter. We used Sierk's [4] angular momentum dependent fission barriers and included a temperature dependence following the parameterization of Newton *et al.* [5]. The fission barrier as well as T_{thresh} were averaged over the angular momentum population distribution leading to fission.

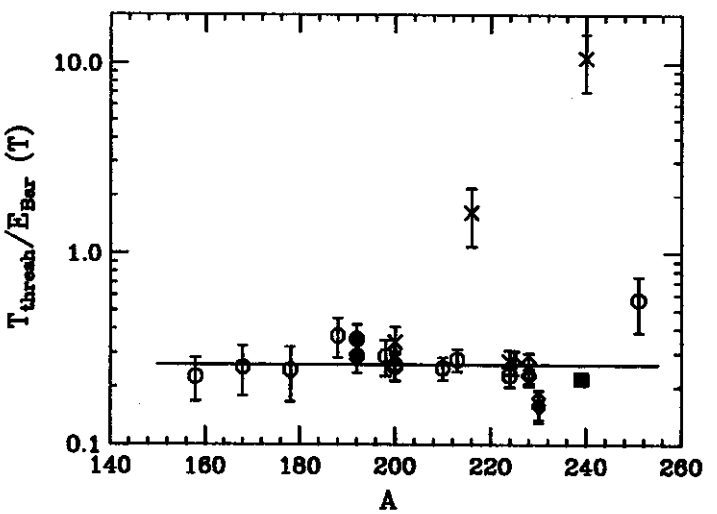

Figure 1: Ratio of the threshold temperature over the average fission barrier as a function of mass for the heavy-ion neutron- (o), proton induced neutron- (□), charged particle-(•) and γ-ray (×) multiplicities and the peripheral collision data (◇). From [3].

Figure 1 shows the ratio $T_{thresh}/E_{Bar}(T)$ as a function of mass of all measured systems [3]. With the exception of two measurements, this quantity seems to be independent of the mass and therefore also

independent of the fissility of the system. Thus, dissipation becomes important when the temperature reaches $\sim$ 20% of the fission barrier. The solid line in Figure 1 corresponds to a fit to the data (excluding the two largest values) and yields a ratio of $T_{thresh}/E_{Bar}(T) = 0.26 \pm 0.05$.

The two data points that do not follow the systematics are from γ-ray measurements following fusion reactions of ^{32}S leading to compound nuclei of ^{216}Th and ^{240}Cf [6]. These are the only reactions of the systematics where the quasi-fission process contributes significantly to the total cross section. In this process the system never penetrates the inner barrier and thus this barrier height can not be a deciding factor in the determination of the onset of dissipation.

Although it is obvious that nuclear dissipation is temperature dependent, the origin of this dependence is still not understood. As Kramers pointed out in his original paper [7], it is far from clear whether the common assumption of a linear friction is justified [8]. Only very recently have calculations attempted to reproduce the excitation dependence of pre-fission evaporation multiplicities as well as fission probabilities [9]. The present observation of a systematic behavior in a wide range of measurements and the existence of a numerical parameter for the onset of dissipation effects is valuable for future theoretical calculations and has to be understood within the models.

a. University of Washington, Seattle, Washington 98195

References

1. D. Hilscher and H. Rossner, Ann. Phys. Fr 17, 471 (1992).
2. P. Paul and M. Thoennessen, Annu. Rev. Nucl. Part. Sci. 44, in press (1994).
3. M. Thoennessen and G. F. Bertsch, Phys. Rev. Lett. 71, 4303 (1993).
4. A. J. Sierk, Phys. Rev. C33, 2039 (1986).
5. J. O. Newton, D. G. Popescu, and J. R. Leigh, Phys. Rev. C42, 1772 (1990).
6. I. Diószegi, *et al.*, Phys. Rev. C 46, 627 (1992), D. J. Hofman, *et al.*, Phys. Rev. Lett. 72, 470 (1994).
7. H.A. Kramers, Physica 7, 284 (1940).
8. M. Nemes and H. Weidenmueller, Phys. Rev. C24 944, (1981).
9. P. Fröbrich, I. I. Gontchar, N. D. Mavlitov, Nucl. Phys. A556, 281 (1993).